

Experimental modeling of algorithms and components for all-optical high-bit-rate digital processors-multipliers using light bullets

A.S. Shcherbakov

*National Institute for Astrophysics, Optics and Electronics,
Phone: 52 (222) 266 3100, ext. 2205; Fax: 52 (222) 247 2940,
e-mail: alex@inaoep.mx*

A. Aguirre Lopez

*Mixteca University of Technology,
Huajuapán de León, Oaxaca, 69000, Mexico,
Phone: 52(953) 532 0399, ext. 500; Fax: 52 (953) 532 0214,
e-mail: aaguirre@mixteco.utm.mx*

Recibido el 12 de agosto de 2005; aceptado el 30 de noviembre de 2006

We present both the estimations of main parameters and the experimental data related to the modeling of algorithms and components for all-optical digital processors-multipliers, exploiting the spatio-temporal optical solitons or light bullets as bit carriers. The modern approach, based on the concept of arranging light beams in space and time using the regime of spatio-temporal solitons is examined from the viewpoint of arresting the collapse of light bullets in a graded-index self-defocusing medium with normal group-velocity dispersion. To perform all-optical computations, the beams of picosecond optical pulses, whose parameters were in one to one coincidence with previously estimated light bullets, have been shaped and employed. Two all-optical algorithms for binary data multiplication in a mixed binary format as well as the corresponding components are designed and experimentally tested with an array of non-collinear second-harmonic generation based optical AND-gates arranged in a square-law optically nonlinear medium.

Keywords: Spatio-temporal soliton; light bullet; all-optical digital multiplication; non-collinear second harmonic generation.

En este artículo se presentan tanto la estimación de los parámetros principales como los datos experimentales en relación al modelaje de algoritmos y los componentes de un procesador-multiplicador digital todo-óptico, explotando los solitones temporales ópticos o balas de luz como portadores de información. Esta moderna aproximación se basa en el concepto de arreglar haces de luz en el espacio y tiempo, usando el régimen de solitones espacio-temporal; estos son examinados desde el punto de vista de detener el desplome de las balas de luz en un medio con índice-graduado de auto-desenfocamiento con dispersión normal de la velocidad de grupo. Para realizar cómputos todo-óptico, se formaron y se emplearon haces de pulsos ópticos de picosegundos de duración, cuyos parámetros coincidían uno a uno con las balas de luz previamente estimadas. Dos algoritmos para la multiplicación todo-óptica de datos binarios en un formato binario mezclado, como también los componentes correspondientes, han sido diseñados y probados experimentalmente con un arreglo de generación de segundo-armónico no-colineal basado en las compuertas-AND ópticas arregladas en un medio óptico no lineal con ley cuadrática.

Descriptores: Solitones espacio-temporal; balas de luz, multiplicación todo-óptica; generación de segundo armónico no colineal.

PACS: 42.65.Pc; 42.65.Re; 42.65.Tg.

1. Introduction

There is great interest in exploiting all-optical devices for digital information processing with a high-bit-rate. Such devices combine the ultrafast parallel processing capabilities of optical systems with the high accuracy of digital computations. The ultimate limit of the processing rate can be anticipated from all-optical parallel architectures that are based on networks of all-optical logic gates using materials exhibiting electronic nonlinearities with response times as low as 10^{-15} second. On the one hand, such a high-bit-rate digital processing needs to invoke the modern concepts based, for example, on the application of spatio-temporal optical solitons or light bullets [1,2] for designing the streams of natural bit carriers. Exploiting light bullets for the purposes of digital data processing may give us, evidently, an opportunity to avoid a few essential difficulties with arranging rather complicated optical schemes and to improve the performance data

of such processors first of all, due to the natural stability of light-bullet bit carriers in space and time. On the other hand, an all-optical digital processor-multiplier may be effectively implemented with an array of non-collinear second-harmonic generation (SHG) based AND logic gates in a crystalline material. Functional capabilities of such a multiplier are determined by the architecture of the array processor. Here, we describe two global algorithms and experimental proof-of-principle results related to the use of the corresponding components for all-optical devices that provide the parallel-input multi-bit digital multiplication, and we discuss other related problems. With the understanding that vector-matrix multiplication is the primary operation, which can be used, for example, to find the unequivalency function and for associative search in a memory system, or can be applied in the basic processor of a digital computing system, we consider the feasibility of exploiting arrays of non-collinear second harmonic generation (SHG) based AND logic gates in bulk materi-

als exhibiting a low-power square-law nonlinearity. For this purpose two opportunities, digital multiplication via the analogue convolution algorithm (DMAC) and the outer-product algorithm [3,4], are inspected theoretically, estimated practically, and tested experimentally. These two cases need rather different post-processing arrangements for the conversion of intermediate mixed-binary format results to a completely binary format. The schemes of components for an all-optical parallel-input processing, data of the experiments carried out, and estimates of potential performance data for the components considered and each of multipliers as a whole, represent the obtained results. To design an extremely high-bit-rate all-optical element for post-processing, it is possible to select a phenomenon that has a fast response time such as, for example, the non-resonant Kerr effect in silica fibers that has a femtosecond response time. However, the post-processing will not be discussed here. To model all-optical computations experimentally, the streams of picosecond optical pulses, whose spatial and temporal widths are into one-to-one correspondence with previously estimated stable light bullets, have been exploited although a graded-index medium has not been yet used at this stage of our experiments. At first, in Secs. 2 and 3, we describe the needed items related to the existence of spatio-temporal solitons in optically nonlinear media from the viewpoint of arresting the collapse of light bullets in a graded-index self-defocusing medium with normal group-velocity dispersion selected for our experimental modeling at this time. In Sec. 4, the algorithms for all-optical parallel-input multiplication are discussed. In the following two sections, 5 and 6, processors based on digital multiplication algorithms via an analogue convolution (DMAC) algorithm and on an outer-product algorithm are considered, including the experimental data. Section 7 represents our concluding remarks related to both theoretical and experimental aspects of the work presented.

2. Spatio-temporal solitons, stable light bullets

Well-known temporal and spatial optical solitons are only special cases of a more general class of nonlinear phenomena in which the spatial and temporal effects are coupled and occur simultaneously. When a pulsed optical beam propagates through a bulk nonlinear medium, it is affected by diffraction and dispersion at the same time and place, and in parallel these two effects become coupled through the medium's nonlinearity. Such a space-time coupling leads to the existence of a group of nonlinear effects, including the formation of light bullets. The starting point for discussion of spatio-temporal solitons is the $(3+1)$ -dimensional nonlinear Schroedinger equation, capable of accounting for the diffractive and dispersive effects occurring simultaneously within the cubic nonlinear medium [5]. For the beginning, it is useful to write this equation in the form

$$i \left(\frac{\partial A}{\partial Z} + \beta_1 \frac{\partial A}{\partial T} \right) + \frac{1}{2\beta_0} \left(\frac{\partial^2 A}{\partial X^2} + \frac{\partial^2 A}{\partial Y^2} \right) - \frac{\beta_2}{2} \frac{\partial^2 A}{\partial T^2} + \gamma |A|^2 A = 0 \quad (1)$$

Physically, $\beta_0 = n_0(\omega_0)k_0$ is the propagation constant, so that $n_0(\omega)$ describes the chromatic dispersion in a medium; $\beta_1 = (d\beta/d\omega)_{\omega=\omega_0} = 1/\nu_g$, where ν_g is the group velocity associated with a pulse; $\beta_2 = (d^2\beta/d\omega^2)_{\omega=\omega_0}$ is the group-velocity dispersion parameter with $\beta = n_0(\omega)\omega/c$ and $k_0 = \omega_0/c$; the nonlinear parameter $\gamma = k_0 n_2$ is responsible for the self-phase modulation due to n_2 , which is the Kerr coefficient. The parameters β_2 and γ , can be positive or negative, depending on the nature of the nonlinear medium. The presence of the above-mentioned effects may lead to shaping optical wave packets that remain confined in all three spatial directions (a finite pulse width corresponds to a finite pulse length along the propagation direction). Such a confined wave packet is often referred to as a light bullet, and it represents an extension of self-trapped optical beams into the temporal domain. To find self-preserving solutions to Eq. (1), it is useful to rewrite it in a normalized form by introducing

$$z = Z / L_D, \quad x = X / w_0, \quad y = Y / w_0, \\ \tau = (T - \beta_1 Z) / \sqrt{L_D |\beta_2|}, \quad u = A \sqrt{|\gamma| L_D}, \quad (2)$$

where $w_0 = (2k_0 |n_1| \beta_0)^{-1/4}$ is the transverse beam width and $L_D = \beta_0 w_0^2$ is the diffraction length. In terms of normalized amplitude u , Eq.(1) can be written as

$$i \frac{\partial u}{\partial z} + \frac{1}{2} \left(\frac{\partial^2 u}{\partial x^2} + \frac{\partial^2 u}{\partial y^2} - (\text{sign}\beta_2) \frac{\partial^2 u}{\partial \tau^2} \right) + (\text{sign}n_2) |u|^2 u = 0. \quad (3)$$

This equation exhibits the total equivalence among the spatial and temporal coordinates when dispersion is anomalous in behavior ($\beta_2 < 0$). One can focus on the anomalous dispersion self-focusing case and exploit this symmetry in solving Eq. (3) with $\text{sign}\beta_2 = -1$ and $\text{sign}n_2 = +1$ Such a restriction is motivated by the fact that, up until now, the stable light bullets have been found in a normal dispersion regime, and maybe even the normal group-velocity dispersion does not permit spatio-temporal localization in the form of light bullets. Let us introduce a three-dimensional vector \mathbf{R} with components x , y , and τ to write Eq. (3) in a compact form

$$i \frac{\partial u}{\partial z} + \frac{1}{2} \nabla_R^2 u + |u|^2 u = 0, \quad (4)$$

where ∇_R^2 is the transversal Laplacian operator. The shape preserving solutions to Eq. (4) can be found by looking for a solution with the property

$$u(x, y, \tau, z) = U(x, y, \tau) \exp(ik_0 z), \quad (5)$$

where k_0 is the propagation constant. Since $U(x, y, \tau)$ does not depend on z , such a pulse would propagate without any

change in its spatial or temporal shape, resulting in an optical bullet. If one writes the Laplacian in Eq. (4) in spherical coordinates and focuses on the radially symmetric solutions, $U(x, y, \tau)$ depends only on $R = \sqrt{x^2 + y^2 + \tau^2}$ and satisfies an ordinary differential equation,

$$\frac{1}{2} \left[\frac{d^2 U}{dR^2} + \frac{(D-1)}{R} \frac{dU}{dR} \right] - k_0 U + U^3 = 0. \quad (6)$$

This equation should be solved with boundary condition $U(R \rightarrow \infty) = 0$. The parameter D takes values 1, 2, or 3 depending on the dimensionality of the vector R . The one-dimensional case ($D = 1$) corresponds to the purely spatial or temporal solitons. The two-dimensional case ($D = 2$) applies to the self-acting beams. The three-dimensional case gives short optical pulses, propagating inside a bulk nonlinear medium, and is related to light bullets. An analytic solution to Eq. (6) in the form $U = \text{sech}R$ can be easily found for $D = 1$, and corresponds to either a spatial soliton ($R = x$) or a temporal soliton ($R = \tau$). For $D > 1$, one can solve this equation only numerically. Of course, the lowest-order solutions are of primary interest, because they reflect optical bullets. Figure 1 shows these solutions by plotting the ratio $U(R)/U(R=0)$ versus the normalized radius R for three cases [1]. The propagation constant k_0 is different in each case: $k_0(D=1) = 0.500$, $k_0(D=2) = 0.206$, and $k_0(D=3) = 0.053$; the peak amplitudes are also different. The stability of any shape-preserving solutions in anomalous dispersion regime should be examined by performing a linear stability analysis. Such an analysis shows that the shape-preserving solution is stable only in the case $D = 1$. When $D > 1$, small fluctuations in the intensity, beam size, or pulse width can grow and lead to spatio-temporal collapse. A consequence of this instability is that, if the pulse energy exceeds a critical value E_0 , the pulse collapses in such a way that the intensity $|u|^2$ becomes infinitely large at a finite distance as the size of a beam diminishes and shrinks to zero both spatially and temporally. The results of numerical solutions to Eq. (6), illustrating the spatio-temporal collapse with $D = 3$ and revealing an important role of the temporal chirp in such a process, are presented in Fig. 2 [6]. The normalized intensity $|U(z, R=0)|^2/U_0^2$ is plotted as a function of the distance z for three values of the normalized initial temporal chirp C . An unchirped pulse with $C = 0$ collapses after a distance $z \approx 0.15$, while the same pulse collapses sooner with $C = +5$ and much later with $C = -5$. Nevertheless, it should be noted that such a conclusion is based on an ideal consideration of the above model.

A few theoretical opportunities have been found for suppressing the collapse via so-called collapse-arresting mechanisms such as self-steepening, saturable nonlinearity, or nonlinear absorption [7]. Moreover, potential perspective exists undoubtedly from the practical point of view. Recent experiments have shown [8,9] that the collapse does not occur in nonlinear Kerr-type media, because of the higher-order effects and that spatio-temporal solitons resembling light bullets can be shaped in a certain range of the optical power.

Here, nevertheless, we shall exclude any higher-order effects which are important already for optical pulses of a width below 1 ps, restrict ourselves by the (3+1)-dimensional equation (3), valid for just a picosecond temporal range, and consider the possibility of arresting spatio-temporal collapse using an inhomogeneous Kerr medium, whose linear part of the refractive index depends on the spatial coordinates.

3. Arresting the spatio-temporal collapse of light bullets

We take a graded-index nonlinear medium whose refractive index can be written as

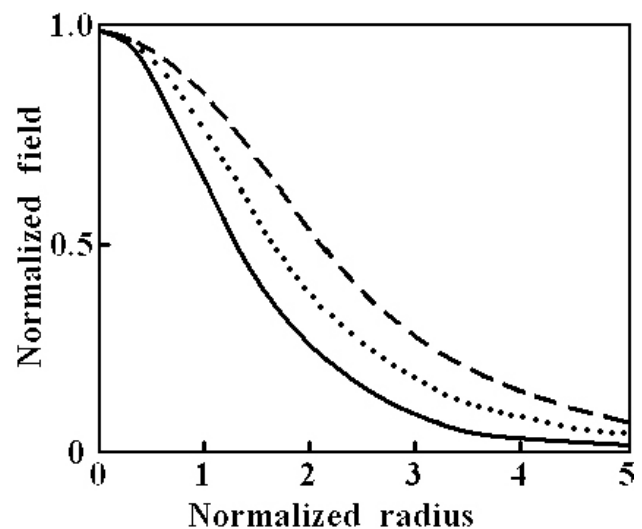


FIGURE 1. Shapes of light bullets inherent in the (3+1)-dimensional nonlinear Schroedinger equation in anomalous group-velocity dispersion regime with: $D = 1$ (solid line), $D = 2$ (dotted line), $D = 3$ (dashed line) [1].

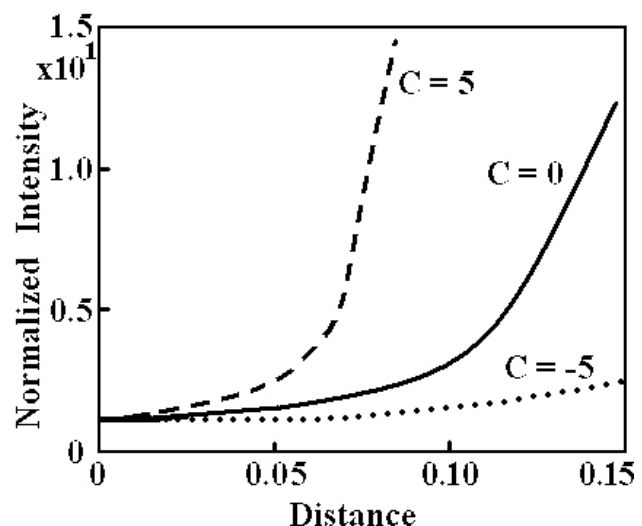


FIGURE 2. Dynamics of collapsing the peak intensity for various chirped Gaussian pulses during their propagation through a Kerr medium with anomalous group-velocity dispersion [6].

$$n(x, y, \omega) = n_0(\omega) + n_1(x^2 + y^2) + n_2|A|^2, \quad (7)$$

where n_1 governs variations in the refractive index in the transverse dimensions x and y reflecting the regimes of guiding ($n_1 < 0$) or anti-guiding ($n_1 > 0$), and n_2 is the nonlinear Kerr coefficient responsible for self-focusing ($n_2 > 0$) or self-defocusing ($n_2 < 0$). Then Eq. (3) can be rewritten as

$$i \frac{\partial u}{\partial z} + \frac{1}{2} \left(\frac{\partial^2 u}{\partial x^2} + \frac{\partial^2 u}{\partial y^2} - (\text{sign}\beta_2) \frac{\partial^2 u}{\partial \tau^2} \right) + \frac{1}{2} (\text{sign}n_1) (x^2 + y^2) u + (\text{sign}n_2) |u|^2 u = 0. \quad (8)$$

Further insight can be gained by using the variational method [10,11], because Eq. (8) can be cast as a variational problem for Lagrangian density

$$\Lambda = \frac{i}{2} \left(u \frac{\partial u^*}{\partial z} - u^* \frac{\partial u}{\partial z} \right) + \frac{1}{2} \left(\left| \frac{\partial u}{\partial x} \right|^2 + \left| \frac{\partial u}{\partial y} \right|^2 \right) - \frac{\text{sign}\beta_2}{2} \left| \frac{\partial u}{\partial \tau} \right|^2 - \frac{\text{sign}n_1}{2} (x^2 + y^2) |u|^2 - \frac{\text{sign}n_2}{2} |u|^4. \quad (9)$$

Noting that the one-dimensional nonlinear Schroedinger equation supports a chirped hyperbolic secant bright soliton in temporal dimension, while a graded-index supports a Gaussian spatial mode with a chirp, an appropriate trial function can be chosen in the form

$$u(x, y, z, \tau) = \sqrt{\frac{E W_T}{2 \pi W_S^2}} \exp \left[-\frac{x^2 + y^2}{2 W_S^2} \right] \text{sech}(\tau W_T) \times \exp [i\phi + iC_S(x^2 + y^2) + iC_T\tau^2], \quad (10)$$

where $E = \int |u|^2 dx dy d\tau$ is the constant pulse energy. The parameters W_S , W_T , C_S , C_T , and ϕ are allowed to be varied with the distance z and represent the spatial and temporal widths, spatial and temporal chirp, and phase associated with a pulse, respectively. One can create the effective Lagrangian $L = \int \int \int \Lambda dx dy d\tau$ and use the Euler-Lagrange equations to obtain a set of evolution equations for these five pulse parameters. The equation for the phase ϕ turns out to be decoupled from the others and can be ignored. The remaining equations are given by

$$\text{a) } \frac{dW_T}{dz} = 2 (\text{sign}\beta_2) C_T W_T, \quad \text{b) } \frac{dW_S}{dz} = 2C_S W_S, \quad (11)$$

$$\lambda = \pm \left\{ W_S \frac{\partial J}{\partial W_S} + W_T \frac{\partial G}{\partial W_T} \pm \sqrt{\left[W_S \frac{\partial J}{\partial W_S} + W_T \frac{\partial G}{\partial W_T} \right]^2 - 4W_S W_T \frac{\partial J}{\partial W_S} \frac{\partial G}{\partial W_T} - \frac{E^2 W_T^4}{3 \pi^4 W_S^6}} \right\}^{1/2}. \quad (15)$$

The spatio-temporal soliton will be stable if λ has no positive real part. It can be seen from Eq. (15) that λ will be purely imaginary when $W_S \frac{\partial J}{\partial W_S} + W_T \frac{\partial G}{\partial W_T} < 0$. Using Eqs. (12) - (14), one can find that

$$W_S \frac{\partial J}{\partial W_S} + W_T \frac{\partial G}{\partial W_T} = -2W_T^2 \left(\frac{6 \pi^2}{E^2} + \frac{4 \pi W_S}{3 E} + \frac{W_T^2}{\pi^2} \right), \quad (16)$$

is indeed negative, and the considered spatio-temporal soliton becomes to be stable.

$$\frac{dC_T}{dz} = 2 (\text{sign}\beta_2) C_T^2 - \frac{2}{\pi^2} W_T^4 (\text{sign}\beta_2) - \frac{E W_T^3}{2 \pi^3 W_S^2} (\text{sign}n_2) \equiv G(C_T, W_T, C_S, W_S), \quad (12)$$

$$\frac{dC_S}{dz} = \frac{1}{2W_S^2} - 2C_S^2 - \frac{E W_T}{12 \pi W_S^4} (\text{sign}n_2) + \frac{(\text{sign}n_1)}{2} \equiv J(C_T, W_T, C_S, W_S). \quad (13)$$

The stationary states corresponding to an optical bullet can be found by setting the z -derivatives to zero. There are two meaningful solutions, both chirp-free due to $C_T = C_S = 0$ [see Eqs. (11)]. One of them ($W_S = 1, W_T = 0$) gives a CW beam. The other one corresponds to the spatio-temporal soliton, whose temporal and spatial widths can be estimated from Eqs. (12) and (13); they are related by

$$\text{a) } W_T = -\frac{E (\text{sign}n_2)}{4 \pi W_S^2 (\text{sign}\beta_2)},$$

$$\text{b) } (\text{sign}n_1) W_S^6 + W_S^2 + \frac{E^2 (\text{sign}\beta_2)}{24 \pi^2} = 0. \quad (14)$$

It can be seen from Eq. (14a) that the medium must have $\text{sign}\beta_2 = -\text{sign}n_2$ to form a stable solution.

Now, to describe our experiments, we focus hereafter only on self-defocusing media with normal group-velocity dispersion and guiding graded index. For such media, we need to take $\text{sign}n_1 = \text{sign}n_2 = -1$ and $\text{sign}\beta_2 = 1$. In this case, there exists a physically meaningful root ($W_S^2 > 0$) of the polynomial equation (14b); in particular it can be estimated by $W_S^2 \approx 1 + E^2 / (48 \pi^2)$ when $E \leq 2\pi$, so that W_T can be found from Eq. (14a) as $W_T = E / (4\pi W_S^2)$. The normalized energy is $E = E_p / E_0$, where the energy scale is defined as $E_0 = \sqrt{|\beta_2|} w_0^2 / (k_0 |n_2| \sqrt{L_D})$.

The stability of this light bullet can be examined by linearizing Eqs.(11) - (13) in terms of small perturbations around the steady-state solution. A linear stability analysis of this type shows that the four eigenvalues λ of a 4×4 - stability matrix are determined by

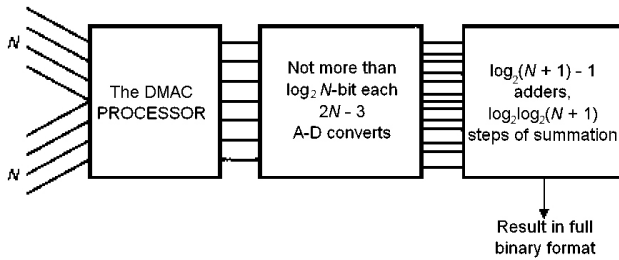


FIGURE 3. Parallel-input N -bit digital multiplication based on the DMAC algorithm.

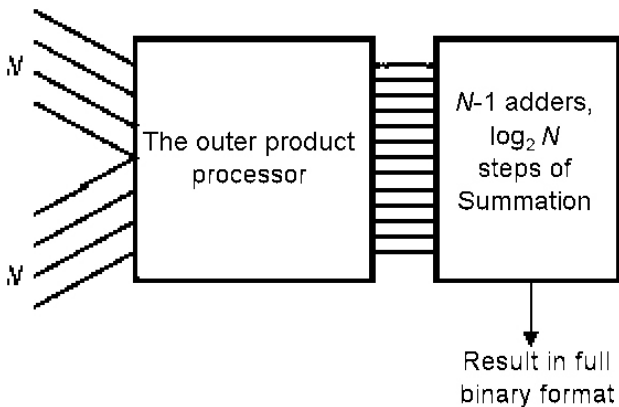


FIGURE 4. Parallel-input N -bit digital multiplication based on the outer-product algorithm.

As an example, one can consider a graded-index glass doped with CdS/Se-semiconductor nanoparticles [12,13]. To estimate the parameters of spatio-temporal solitons for such a medium we assume an operating wavelength near $1 \mu\text{m}$ where $\beta_2 \approx 50 \text{ ps}^2/\text{km}$ is positive, while $n_2 \approx -10^{-16} \text{ m}^2/\text{W}$ is negative. The negative waveguiding parameter n_1 sets the beam-size scale w_0 and can be varied over a wide range. Let us take $w_0 = 1 \text{ mm}$ and $n_0 = 1.45$, so that $\beta_0 \approx 9 \mu\text{m}^{-1}$ and $L_D \approx 0.9 \text{ m}$. The energy scale E_0 will be 400 pJ , and the spatial and temporal widths of the optical bullet are thus around $X_0 \approx 1 \text{ mm}$ and $T_S = 8.5 \text{ ps}$, respectively. The formation of a stable light bullet in this Kerr medium is guaranteed by the inhomogeneous nature of the nonlinear medium. From now on, we will use these estimates, bearing in mind the experimental modeling of various all-optical computations in the spatio-temporal soliton regime.

4. Algorithms for all-optical parallel-input digital multiplication

Vector-matrix multiplication is the primary operation which is exploited, for example, in finding the unequivalency function for an associative search in a memory system or which is applied in the central processor of a digital computer. All-optical components for multiplication can be implemented by using various nonlinear phenomena via non-collinear SHG in square-law nonlinear crystalline material [14]. Depending on the algorithm, two architectures for parallel-input digital

multiplication can be considered, namely the DMAC and the outer-product processors. These two cases need rather different post-processing arrangements for analogue-to-digital conversion of intermediate mixed-binary format results to a binary format. Schematic arrangements for the DMAC and outer-product processors are presented in Figs. 3 and 4, respectively. These figures show that the DMAC algorithm requires a smaller number, $\log_2(N+1) - 1$, of adders and a smaller number, $\log_2 \log_2(N+1)$, of summation steps, but the need for analogue-to-digital conversion limits the application of this algorithm. The outer-product algorithm requires a greater number, $N - 1$, of parallel adders, achieving summation in a greater number, $\log_2 N$, of steps. However, in the alternative case there is no analogue-to-digital conversion, which seems to be preferable for the creation of all-optical components because it preserves the binary format and so removes a dynamic range problem.

The full adder is the key component in all-optical post-processing of intermediate results. Such an adder may be designed to use only the basic AND and EXCLUSIVE-OR logic gates, so implementation of a multiplier is conditioned by the feasibility of realizing high-speed all-optical logic gates. It is well-known that performing, for example, NOR and NAND logic operations as well as creating AND and NOT or NOT and OR logic gate pairs is sufficient for the arrangement of any arithmetic device, in particular for binary number multipliers. To achieve an extremely high speed of operation and ease of fabrication, it seems to be more promising first to obtain results in an intermediate mixed-binary format by a DMAC, or an outer-product processor, and then to convert that signal to a completely binary format. The non-resonant Kerr effect is an ultrafast phenomenon that permits switching times as low as 10^{-15} second, and makes possible an extremely high rate of logic operations in comparison with digital electronic signals. An application of ultrafast response requires an abnormally high intensity of light beams and the problem of heat removal becomes more complicated for the high density of information in the data flow. For this reason, the optical Kerr effect proves to be acceptable for computing first of all in low-loss optical fiber, because the heat power, given its small value, dissipates lengthwise along the optical fiber and does not lead to any difficulties even for the top speed of operation. However, the weak Kerr nonlinearity manifests itself only in a long length of fiber, so the output signal has a market time delay relative to the input signal. This time delay, nevertheless, should not be regarded as a considerable demerit for optical fiber components, because the data flow arrangement is such that performing each of the following operations does not depend on the results of all the previous processing operations.

5. All-optical processing based on the DMAC-algorithm

At first, shaping the DMAC signal via a non-collinear SHG-phenomenon in square-law optically nonlinear crystalline

material is presented. The diagram of a non-collinear SHG-phenomenon may be considered an all-optical AND logic gate. Such a gate has a femtosecond time response and does not need an optical pump beam, so that a widely branched network of coupled gates with repeated use of initial light beams may be implemented, because only a small part of the input signal energy is converted into the SHG output signals. In fact, each of the partial interactions corresponds to an undistributed field approximation. The light beam arrangement for the DMAC-algorithm signal shaping is shown in Fig. 5.

Binary numbers are encoded by a total of N parallel optical channels, one channel for each of the N bits that comprise the following numbers:

$$A = \sum_{i=0}^{N-1} a_i 2^i \quad \text{and} \quad B = \sum_{i=0}^{N-1} b_i 2^i.$$

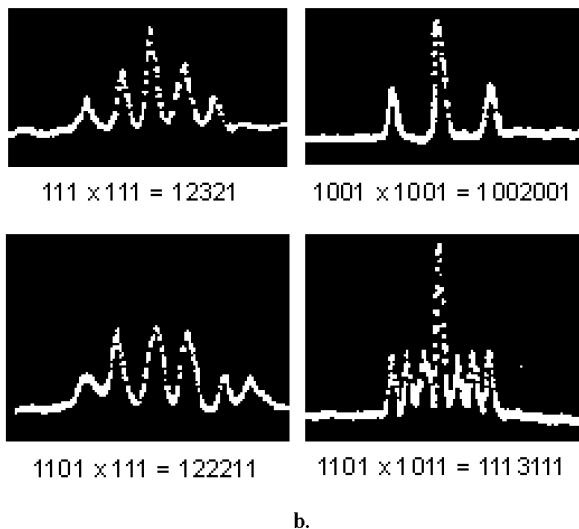
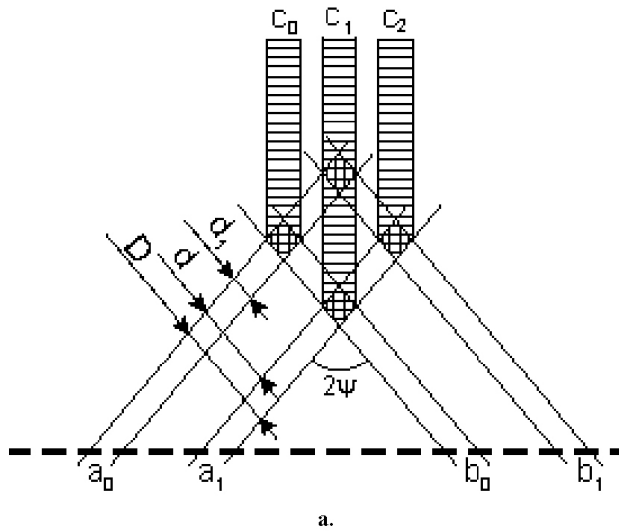


FIGURE 5. (a) Configuration of AND logic gates totally performing DMAC; (b) Experimental results: all-optical shaping of the DMAC-signals.

Intensities of light beams have magnitudes equal to 0 or 1 in both these channels. There are N^2 areas of non-collinear interaction in a crystal when initial light beams pass through a crystal under a phase-matching condition. Similar areas play the parts of partial multipliers or AND logic gate networks, which are integrated into a single crystal. By providing an equidistant arrangement of the input optical channels, the intensities of the second-harmonic light beams are summed up along diagonal lines, so $(2N + 1)$ parallel output channels prove to be shaped in the output plane. That is to say, the signals leaving the network arrangement are exactly the partial DMAC-signals:

$$c_i = \sum_{j=0}^{N-1} a_j b_{i-j},$$

and consequently,

$$C = AB = \sum_{i=0}^{2N-2} c_i 2^i. \tag{17}$$

In view of simultaneous arrival of optical pulses at each of the interaction areas, the initial optical beam fronts need to be sloped as shown in Fig.5a. Both the intensity depletion of the initial signals as a result of repeated interaction in the convolution network and the diffraction of the optical beams have an effect on the number of bits, N , that can be handled in the processing of binary numbers. It may be shown that, on the one hand, for the processing of 32-bit numbers, the efficiency of the individual partial interactions ought to be no greater than 1% and, on the other hand side, the maximal value of bits N_{max} is limited by diffraction to

$$N_{max} = \sqrt{\frac{n_A D \sin 2\Psi}{8 \lambda_0}}, \tag{18}$$

where λ_0 is the wavelength of the initial light beams, n_A is the average refractive index for a crystal, and D is the geometric size, which is shown in Fig. 5a. In the spatio-temporal soliton regime, this restriction can be omitted and the value $N = 32$ bits may be taken. The speed of operation is usually described by the time T for one operation performing as well as by the productivity S , i.e. the maximal number of bit operations in unit time:

$$T = \frac{2n_A D}{c \sin 2\Psi} + \tau, \quad S = \frac{N^2}{\Delta T + \tau}, \tag{19}$$

where c is the velocity of light, τ is the bit pulse width, and ΔT is the spreading time. The productivity S is defined by the maximum attainable frequency of data input into the operations, which is limited in its turn by the following factors:

- a) the time response of the logic gates;
- b) the bit pulse width;
- c) the path time of one bit multiplication area; and
- d) non-simultaneous responses of the logic gates in a convolution network.

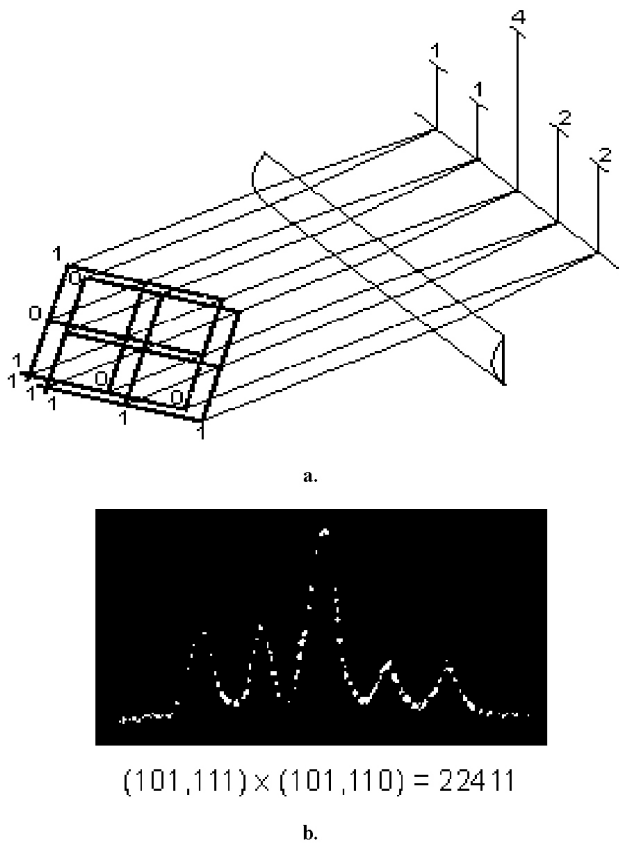


FIGURE 6. (a) The DMAC-signal shaping in the case of the inner product of vectors: (a) a schematic of 2-component 3-bit vectors; (b) experimental result $(101, 111) \times (101, 110) = 22411$.

The last factor gives the main limitation, which is why the greatest spreading time ΔT has a signal on the central diagonal line due to the response non-simultaneity

$$\Delta T = \frac{D}{c \sin 2\Psi} \left(\frac{n_0^\omega}{\cos \Psi} - n_0^{2\omega} \right), \quad (20)$$

where n_0^ω and $n_0^{2\omega}$ are the refractive indexes for the input beams and the SHG-beams, respectively. For example, at $\lambda_0 = 1060$ nm, with $\tau = 1$ ps and $N = 32$, one can obtain $\Delta T = 16$ ps and $S = 6 \times 10^{13}$ bit/s in a LiJO_3 single crystal.

A three-dimensional network of logic gates, formed by M planes of interaction as that depicted in Fig. 5a, permits digital inner vector multiplication in mixed-binary format for M -component vectors with N -bit components using an output cylindrical lens (see Fig. 6a). The number M of vector components which can be accommodated within a given crystal thickness H is determined by Eq. (18). For instance, it is possible to have $M = 32$ when $H = 8$ mm in a LiJO_3 single crystal even in the regime free of spatio-temporal solitons. The inner-product processor productivity is equal to $S = M N^2 (\Delta T + \tau)^{-1}$; so for $M = N = 32$ and $\tau = 1$ ps, one can get $\Delta T = 16$ ps and $S = 2 \times 10^{15}$ bit/s.

In the experiments, a LiJO_3 plate has been used with dimensions $27 \times 27 \times 8$ mm cleaved in the (100) crystallographic plane with the input facet orthogonal to the [010]

axis, so $\Psi = 20^\circ$ and $D = 8$ mm. Experimental simulation of the input optical signals with $N = 4$ for each of the binary numbers was made by symmetrical diaphragm masks ($d = 1.6$ mm, $d_1 = 0.8$ mm). The light source generated 7 ps width pulses at $\lambda_0 = 1060$ nm. These parameters of the optical pulse stream have been selected as rather close to the parameters of light bullets discussed in section 3 to provide experimental modeling of exploiting the spatio-temporal optical solitons in all-optical computations. Optical signals of the second-harmonic beams were detected by means of a multiple-point photodetector, so the DMAC signals have been displayed, see Fig. 5b. The time T to perform one operation was equal to 130 ps, which corresponded to $\Delta T = 17$ ps and $S = 6 \times 10^{11}$ bit/s. The vector inner-product signal in mixed-binary format is presented in Fig. 6b. This is the case for the multiplication of two-component vectors ($M = 2$) with three-bit components ($N = 3$). The same masks were again exploited, $D = 5$ mm. The values of $\Delta T = 10$ ps and $S = 1 \times 10^{12}$ bit/s have been achieved.

Optical parallel analogue-to-digital conversion can be simplified by designing the logic network with a different spatial period of the input channels for both binary numbers. Figure 7 illustrates the process where the number of optical pulses of equal amplitudes in each position quantifies the magnitudes of binary convolution partial products. Therefore, in post-processing, the analogue-to-digital converters must be replaced with pulse counters in all the mixed-binary format positions. In this spatially irregular case, the maximum number of multiplicand bits has an order of magnitude equal to the square root of N_{\max} given above by Eq. (1) or it can be 32 bits in the spatio-temporal soliton regime, if the efficiency of an individual interaction is about 1% or even less. Other masks for the bits ($d_1 = 0.5$ mm, $d_2 = 3.0$ mm, $d_3 = 2.0$ mm, $N = 3$) were exploited in the next experiment (see Fig. 7a). The corresponding oscilloscope traces are shown in Fig. 7b.

On the whole, spatially irregular analogue-to-digital conversion can be successfully applied to mixed-binary format processing only if the number of multiplicand bits is not very large. The response non-simultaneity $\Delta t = \Delta T N^{-1}$ of signal arrivals from neighboring logic gates placed on the same diagonal line may be used for mixed-binary format analogue-to-digital signal conversion as well. For the case $\tau < \Delta t$, the time resolution of pulses, which are shaping a mixed-binary format signal, proves to be attainable. The condition $\tau < \Delta t = 3.5$ ps was achieved in the experiment described above with $d = 1.6$ mm.

6. All-optical processing based on the outer-product algorithm

Digital information processing includes the outer-product operation, so several algorithms of linear algebra can be based on this operation. The outer-product multiplication of two N -dimensional vectors A and B is given by

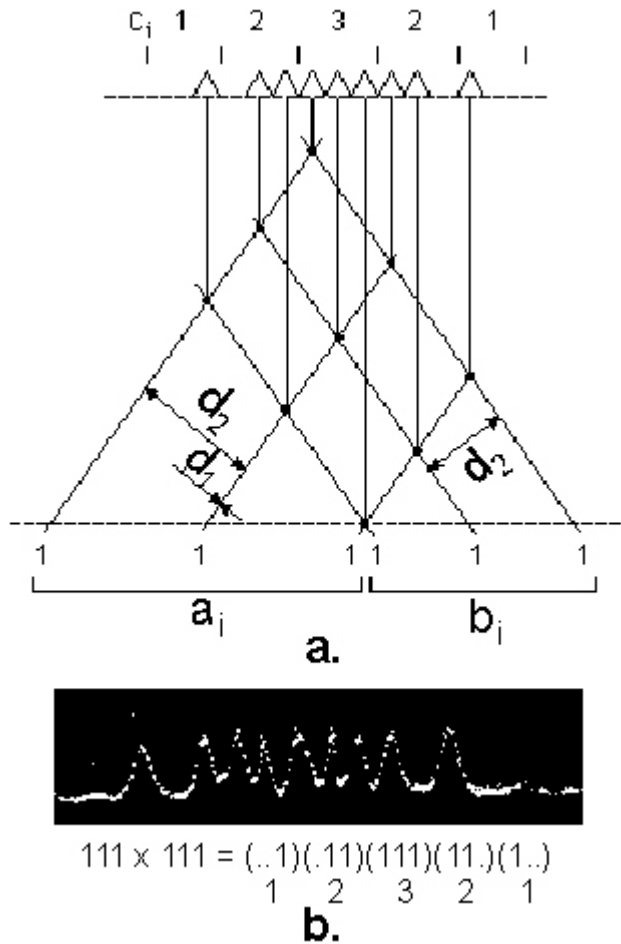


FIGURE 7. Spatially irregular case of an AND logic gates network: (a) schematic arrangement; (b) experimental result of multiplication: $111 \times 111 = 12321$.

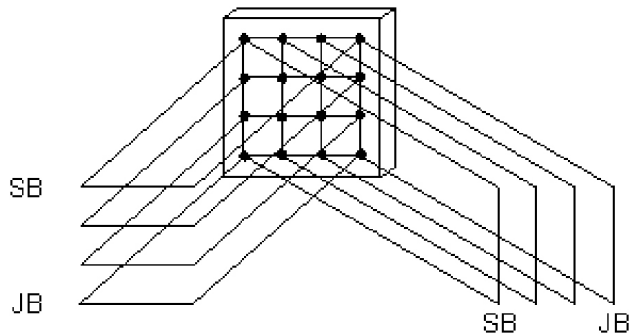


FIGURE 8. A scheme of the outer-product processor; SB are the senior bits of a number, JB are the junior bits.

$$C = AB^T = \begin{pmatrix} a_1 b_1 & \dots & a_1 b_N \\ \dots & \dots & \dots \\ a_N b_1 & \dots & a_N b_N \end{pmatrix}, \quad (21)$$

where C is an $N \times N$ matrix containing only one linearly independent line or column. In the case of processing binary data, the outer-product operation is reduced to a shaping of the partial product matrix, which consists of N^2 optical signals having intensity magnitudes equal to 0 or 1. The prin-

ciple of such a matrix processor arrangement is presented in Fig. 8.

Light beams, corresponding to binary numbers bits, are collimated in a vertical or horizontal plane and are then they are directed at the input facet of a nonlinear crystal for SHG under the phase matching condition. The interaction of non-collinear optical beams takes place in a crystal where the full totality of partial products is carried out. In fact, the matrix of the SHG signals is the outer product of the initial vectors with one-bit components. The nonlinear crystal plate thickness must be optimal so that all interaction areas of the first row are placed inside the plate, with no following interactions taking place. The optimal thickness of the LiJO_3 crystal cleaved in the (100)-plane as a 30×30 mm sized plate was equal to 1.2 mm for the partial product generation of 32-bit binary numbers. The number of bits is connected solely with the quality and geometric size of the plate and with the capabilities of shaping the input optical signals. Productivity S of such a processor is determined by a minimal period T of operating on digital data, which is conditioned in its turn by a time response of partial logic gates. One can obtain $S = N^2 T^{-1}$, so for $N = 32$, and $T = 1$ ps we get $S = 1 \times 10^{15}$ bit/s.

The parallel-input outer-product processor based on the SHG-gate network was built experimentally with the input light beams collimated in orthogonal directions, encoded with binary data, and a plate of LiJO_3 single crystal placed perpendicularly to the plane of interaction. An array of 4×4 binary products was generated in such a network using four-channel masks and 7 ps optical pulses at $\lambda_0 = 1060$ nm, being close to the parameters of light bullets estimated in Sec. 3. After using a cylindrical lens to sum the SHG-signals over diagonal lines of the matrix, a seven-bit product in mixed-binary format was obtained. Experimental results of binary number multiplication by such a processor are shown in Fig. 9.

The absence of limitations connected with light intensity exhaustion, diffraction of beams, and response non-

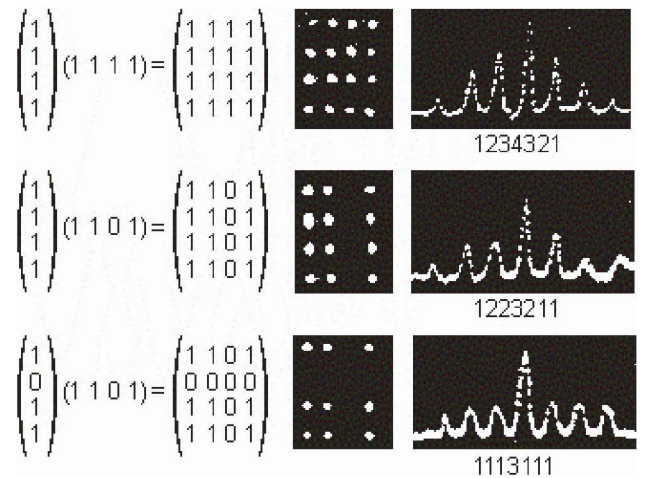


FIGURE 9. Results of multiplication using an all-optical outer-product processor.

simultaneity is an advantage of the outer-product multiplier as compared to the DMAC-processor. At the same time, the outer-product multiplier contains additional optics and is not capable of operating with vectors having multibit components because of a three-dimensional schematic arrangement. On the whole, the outer-product multiplier seems to be the most promising, because it needs in addition to the matrix processor only two homogeneous components, namely, EXCLUSIVE OR and AND logic gates. This property of the outer-product processor (see Fig.4) can turn out to be decisive since at present it is still not known how to produce an extremely high-bit-rate all-optical analogue-to-digital converter.

7. Conclusion

In view of parallel-input multiplication, both the DMAC and the outer-product algorithm could be exploited for primary binary data processing. The schemes, which use optical SHG techniques for performing binary multiplication, have been considered and proof-of-principle experiments have been carried out. Estimations have shown that, through pipelining of data in an optical network produced in nonlinear crystals, the processing of 32-bit numbers is possible for a bit rate of up to 10^{15} bit/s and an optical energy consumption for each individual logic AND operation down to a value of 10^{-12} J/bit. The DMAC-algorithm based device needs an analogue-to-digital converter or pulse counter in the irregular arrangement case. The outer product multiplier is free of some of the flaws enumerated above, but its three-dimensional set does not per-

mit operation by vectors, in contrast to the DMAC multiplier. In any event, an all-optical full adder is the key component of post-processing in such devices, so the problem of implementing logic gates becomes significant. For this purpose, for instance, optical fiber ultrafast logic devices based on Kerr nonlinearity in Sagnac-effect interferometric configurations can be applied.

These feasibilities for applications to an all-optical digital processing can be really improved due to operation in the regime of spatio-temporal solitons representing optical bullets. In this case, the negative influence of light diffraction will be compensated by the corresponding index-graded contribution, while the width of bit pulses will be stabilized because of the balance between dispersion and nonlinearity. Recent experiments have shown that the possibility of shaping the light bullets in a certain range of the optical power is hardly practical. From the viewpoint of further applications, optical bullets will be able to play the role of natural ultrashort bit carriers, well localized in space and time, whose parameters are matched by the properties of the materials exploited. Such a statement of the problem for designing the processor architecture permits potentially optimizing of both the schematic arrangement and the functional components of an all-optical high-bit-rate processor-multiplier.

Acknowledgments

This work was financially supported by the CONACyT (Project # U 41998-F).

-
1. Y. Silberberg, *Opt. Lett.* **15** (1990) 1282.
 2. R. McLeod, K. Wagner, and S. Blair, *Phys. Rev. A* **52** (1995) 3254.
 3. J.W. Goodman, *Introduction to Fourier Optics*, 2-nd Ed. (McGraw Hill)
 4. F. Yu. *Introduction to Information Optics* (Academic Press, San Diego, 2001).
 5. G.P. Agrawal, *Nonlinear Fiber Optics*, 2-nd Ed. (Academic Press, San Diego, 1995).
 6. X.D. Cao, C.J. McKinstrie, and G.P. Agrawal, *Phys. Rev. A* **49** (1994) 4085.
 7. Y.S. Kivshar and G.P. Agrawal, *Optical Solitons: From Fibers to Photonic Crystals* (Academic Press, Amsterdam, 2003).
 8. X. Liu, L.J. Qian, and F.W. Wise, *Phys. Rev. Letters* **82** (1999) 4631.
 9. H.S. Eisenberg *et al.*, *Phys. Rev. Letters*. **87** (2001) 1.
 10. N.N. Akhmediev and A. Ankiewicz, *Solitons: Nonlinear Pulses and Beams* (Chapman & Hall, London, 1997).
 11. S. Raghavan and G.P. Agrawal, *Opt. Commun.* **180** (2000) 377.
 12. E. Donkor and R. Boncek, *Proc. SPIE* 3075 (1997) 166.
 13. D. Mayweather, M.J.F. Digonnet, and R.H. Pantell, *IEEE Journ. Lightwave Tech.* **14** (1996) 601.
 14. H.A. Haus, *Waves and Fields in Opto-Electronics* (Prentice Hall, Upper Saddle River, 1984).